Mechanisms of disease

Cytosolic β-amyloid deposition and supranuclear cataracts in lenses from people with Alzheimer's disease

Lee E Goldstein, Julien A Muffat, Robert A Cherny, Robert D Moir, Maria H Ericsson, Xudong Huang, Christine Mavros, Jennifer A Coccia, Kyle Y Faget, Karlotta A Fitch, Colin L Masters, Rudolph E Tanzi, Leo T Chylack Jr, Ashley I Bush

Summary

Background Pathological hallmarks of Alzheimer's disease include cerebral β-amyloid (Aβ) deposition, amyloid accumulation, and neuritic plaque formation. We aimed to investigate the hypothesis that molecular pathological findings associated with Alzheimer's disease overlap in the lens and brain.

Methods We obtained postmortem specimens of eyes and brain from nine individuals with Alzheimer's disease and eight controls without the disorder, and samples of primary aqueous humour from three people without the disorder who were undergoing cataract surgery. Dissected lenses were analysed by slit-lamp stereophotomicroscopy, western blot, tryptic-digest/mass spectrometry electrospray ionisation, and anti-Aβ surface-enhanced laser desorption ionisation (SELDI) mass spectrometry, immunohistochemistry, and immunogold electron microscopy. Aqueous humour was analysed by anti-Aβ SELDI mass spectrometry. We did binding and aggregation studies to investigate Aβ-lens protein interactions.

Findings We identified Aβ1–40 and Aβ1–42 in lenses from people with and without Alzheimer's disease at concentrations comparable with brain, and Aβ1–40 in primary aqueous humour at concentrations comparable with cerebrospinal fluid. Aβ accumulated in lenses from individuals with Alzheimer's disease as electron-dense deposits located exclusively in the cytoplasm of supranuclear/deep cortical lens fibre cells (n=4). We consistently saw equatorial supranuclear cataracts in lenses from people with Alzheimer's disease (n=9) but not in controls (n=8). These supranuclear cataracts colocalised with enhanced Aβ immunoreactivity and birefringent Congo Red staining. Synthetic Aβ bound αB-crystallin, an abundant cytosolic lens protein. Aβ promoted lens protein aggregation that showed protofibrils, birefringent Congo Red staining, and Aβ/αB-crystallin coimmunoreactivity.

Interpretation Aβ is present in the cytosol of lens fibre cells of people with Alzheimer's disease. Lens Aβ might promote regionally-specific lens protein aggregation, extracerebral amyloid formation, and supranuclear cataracts.

Lancet 2003; **361:** 1258–65

Laboratory for Oxidation Biology (L E Goldstein MD, J A Muffat MS, X Huang PhD, J A Coccia AB, K Y Faget AB, A I Bush MD)**, Genetics and Aging Research Unit** (L E Goldstein, J A Muffat, R D Moir PhD, X Huang, J A Coccia, K Y Faget, Prof R E Tanzi PhD, A I Bush)**, Massachusetts General Hospital, Charlestown, MA 02129, USA; Center for Ophthalmic Research, Brigham and Women's Hospital, Boston, MA 02115, USA** (L E Goldstein, J A Muffat, Prof L T Chylack Jr MD)**; Department of Psychiatry** (L E Goldstein, J A Muffat, X Huang, A I Bush)**, Department of Neurology** (R D Moir, R E Tanzi)**, and Department of Pathology** (K A Fitch BS)**, Massachusetts General Hospital, Boston, MA 02114, USA; Ecole Normale Superieure, Department of Bioengineering, Cachan, France** (J A Muffat)**; Mental Health Research Institute of Victoria and Department of Pathology, University of Melbourne, Australia** (R A Cherny PhD, C Mavros BS, Prof C L Masters MD, A I Bush)**; and Harvard Medical School Electron Microscope Facility, Boston, MA 02115, USA** (M H Ericsson BS)

Correspondence to: Dr Ashley I Bush, Laboratory for Oxidation Biology, Genetics and Aging Research Unit, Massachusetts General Hospital, Building 114, 16th Street, Charlestown, MA 02129-4404, USA (e-mail: bush@helix.mgh.harvard.edu)

Introduction

Pathogenesis of Alzheimer's disease is characterised by age-dependent cerebral deposition of β-amyloid (Aβ) peptides, which are 39–43 aminoacid residues long and are generated by endoproteolytic cleavage of the β-amyloid precursor protein (β-APP). The Aβ1–42 isoform is enriched in neocortical deposits,[1] is overproduced in people with familial Alzheimer's disease,[2] and contributes to disease-associated oxidative stress, protein aggregation, and neurotoxic effects.[3]

The human lens is also vulnerable to age-dependent degenerative changes and shows progressive deposition of insoluble protein and extensive oxidative damage.[4,5] Early-onset cataracts and Alzheimer's disease are typical comorbid disorders in adults with Down's syndrome[6] and in those with familial Danish dementia,[7] an Alzheimer's disease variant with cerebral Aβ amyloidosis. Evidence shows that Aβ is expressed in rodent and monkey lens.[8] Conversely, αB-crystallin—an abundant cytosolic lens protein and small heat-shock protein with MOLECULAR CHAPERONE properties[9]—is expressed in brain of individuals with Alzheimer's disease.[10] Moreover, Aβ interacts with αB-crystallin in vitro[11,12] and in Aβ-expressing transgenic *Caenorhabditis elegans*.[13]

Despite speculation[8,14,15] about the possibility of overlapping Alzheimer's disease-associated molecular pathological findings in the lens and brain of people with this disorder, to our knowledge, no study to date has investigated this hypothesis in man. Thus, we aimed to investigate this hypothesis.

Methods

Samples

The study adhered to hospital regulations, national laws, and the Declaration of Helsinki. Procurement of tissue specimens for this study was approved by institutional review boards at the Massachusetts General Hospital and the Massachusetts Eye and Ear Infirmary, Boston, MA, USA. We obtained informed consent for research use of the brain and both eyes from next-of-kin relatives. Lenses were dissected from intact globes obtained

GLOSSARY

ELECTROSPRAY IONISATION MASS SPECTROMETRY
Analytical technique for the study of large molecules, especially proteins and peptides. The technique derives detailed information about molecular weights and structures from very small sample quantities. Electrospray ionisation refers to the methods by which the molecule under analysis is charged, or ionised. In this technique, charged droplets are generated by spraying the sample solution under a strong electric field. Ionisation occurs by protonation to produce gas-phase macromolecular ions directly from solution. The ionised molecule is then injected into a mass spectrometer to precisely determine the molecular mass/charge ratio.

MOLECULAR CHAPERONE
Molecular chaperones are cellular proteins that assist in the establishment and maintenance of proper protein folding, a requirement for normal protein function. In addition to promotion of correct protein folding, molecular chaperones prevent aberrant protein interactions and help stabilise cellular proteins against unfolding induced by age, heat, oxidants, or ultraviolet light. Examples of molecular chaperones include heat shock proteins. These are highly conserved proteins that are expressed in both prokaryotic and eukaryotic cells when those cells are stressed by environmental conditions, such as exposure to certain chemicals, pathogens, or heat; examples of heat shock proteins are HSP70, HSP90, and the small heat shock protein family that includes HSP27 and αB-crystallin.

REVERSED-PHASE HIGH PERFORMANCE LIQUID CHROMATOGRAPHY (RP-HPLC)
A liquid partition chromatography analytical chemistry technique. A stationary phase consisting of very small non-polar particles packed in a column is used with a polar liquid mobile phase (reversed phase) to fractionate polar solutes. Polar molecules will elute from a particular column/mobile phase combination with a characteristic retention time, thus facilitating chemical characterisation. Various detection methods (eg, fluorescence, electrochemical) are available to quantitatively assess compounds as they are eluted from the column.

TANDEM MASS SPECTROMETRY
Analytical technique involving serial mass spectrometric analyses of a protein or peptide with intervening molecular fragmentation in a collision chamber. This analysis permits mass/charge comparison before and after fragmentation, thus providing a means for determination of aminoacid composition. When used in combination with trypsinisation or other enzymatic digestion of an unknown protein sample, tandem mass spectrometry permits precise aminoacid sequencing and specific identification of small quantities of protein.

TBOC CHEMISTRY
Method for peptide synthesis that involves use of tert-butyloxycarbonyl (tBOC) to block amino groups during successive cycles of aminoacid addition.

THIOFLAVIN FLUORESCENCE ANALYSIS
The fluorochromic dyes and thioflavin-S thioflavin-T fluoresce when bound to amyloid or protein that assumes an amyloid-like structure. Thioflavin dyes interact with the quartenary structure of the β-pleated sheet, rather than with specific aminoacid sequences or moities. Thioflavin dyes are not specific for amyloid and can react with other cellular components, including fibrinoid, arteriolar hyaline, keratin, and zymogen granules.

through collaborative arrangement with the Massachusetts Alzheimer's Disease Research Center, Boston, MA, USA. All lens specimens used in this study did not have traumatic, morphological, or cold-storage artifacts. Comprehensive neuropathological examinations were done in accordance with established procedures and assessed by CERAD (consortium to establish a registry for Alzheimer's disease) criteria.[16]

We obtained primary aqueous humour samples from consenting adult volunteer patients who did not have Alzheimer's disease and who were undergoing routine cataract extraction at the Massachusetts Eye and Ear Infirmary. We took samples of anterior chamber fluid at the beginning of intraocular surgery with a sterile 0·5 mL tuberculin syringe and froze these at –80°C until analysis.

Procedures

Peptide synthesis

Human Aβ peptides (Aβ1–40, Aβ1–42) were commercially synthesised by TBOC CHEMISTRY and purified by chromatography on a preparative C-18 or C-4 REVERSED-PHASE HIGH PERFORMANCE LIQUID CHROMATOGRAPHY (RP-HPLC) system (at the W M Keck Foundation Biotechnology Resource Laboratory, Yale University Medical School, New Haven, CT, USA). Lot purity (>98%) was assessed by mass spectrometry and composition by aminoacid analysis. We received gifts of purified recombinant human αB-crystallin (J Liang, Brigham and Women's Hospital, Boston); rabbit polyclonal antibodies raised against human αB-crystallin (J Liang; J Horwitz, UCLA School of Medicine); and mouse monoclonal antibody WO2 raised against Aβ5–8 (C Masters). We purchased as purified IgG monoclonal antibodies against Aβ (6E10 [Aβ1–17] and 4G8 [Aβ17–24]; Signet Laboratories, Dedham, MA; and βA4 [Aβ8–17]; Dako, Carpenteria, CA, USA) and against β-APP (22C11 [N-terminal β-APP66–81]; Research Diagnostics, Flanders, NJ, USA; A8717 [C terminal β-APP676–695]; Sigma, St Louis, MO, USA). We determined protein concentrations by the bicinchoninic acid method (Pierce, Rockford, IL).

Lens classification

Dissected lenses were bathed in 37°C isotonic medium TC-199 (Invitrogen, Carlsbad, CA, USA), illuminated with a slit-lamp apparatus attached to a Zeiss OPMI-1 surgical stereophotomicroscope (Carl Zeiss, Thornwood, NY, USA) fitted with a Zeiss-Urban stereoscopic beam-splitter (Urban Engineering, Burbank, CA, USA), and graded in accordance with Cooperative Cataract Research Group criteria[17] by a skilled rater masked to clinical history and neuropathological diagnoses.

β-APP purification and western blots

We homogenised tissues in ice-cold phosphate-buffered saline and ultracentrifuged the samples at 100 000 *g* for 1 h at 4°C. The pellet was retained as membrane extract. We adjusted the salt concentration to 350 mmol/L NaCl pH 8, and applied the extract to Macro-Q anion exchange resin (Pharmacia, Peapack, NJ).[18] Samples were eluted with 1 mol/L NaCl in 50 mmol/L Tris pH 8·0, blotted, and probed for β-APP with monoclonal antibody 6E10, which detects an epitope in the Aβ region of β-APP. The identity of detected bands as β-APP was conferred by affinity purification, 6E10 immunoreactivity, and SDS-PAGE migration consistent with purified β-APP (110 and 130 kD). We homogenised lyophilised lenses in ice-cold phosphate-buffered saline and ultracentrifuged them at 100 000 *g* for 1 h at 4°C. The soluble or urea-resolubilised pellet fractions were standardised for protein concentration and equal volumes were electrophoresed on Tris/tricine-polyacrylamide gels and western blotted. We detected Aβ with mouse monoclonal antibody WO2 and analysed the western blots by densitometry.[19]

Tryptic digest sequencing and electrospray ionisation mass spectrometry

We prepared lens homogenate as described above and ultracentrifuged it. The supernatant and urea-resolubilised pellet fractions were dissolved separately in sample buffer containing 8 mol/L urea, heated, electrophoresed on 10–20% Tricine gels, and stained with Coomassie blue. A discretely staining, roughly 4 kD, Coomassie-detectable

band was excised, minced, and subjected to in-gel trypsinisation. We fractionated extracted peptides by RP-HPLC and subjected them to ELECTROSPRAY IONISATION MASS SPECTROMETRY and LCQ-DECA ion-trap mass spectrometry (ThermoFinnigan, San Jose, CA). Eluting peptides were isolated and fragmented by TANDEM MASS SPECTROMETRY. We identified peptide sequences by a computer search program (Sequest, ThermoFinnigan) that matches the acquired fragmentation pattern to known proteins.

Surface-enhanced laser desorption ionisation mass spectrometry

We incubated human lens protein extracts or primary aqueous humour samples on a surface-enhanced laser desorption ionisation (SELDI) mass spectrometry protein array chip (Ciphergen Biosystems, Fremont, CA, USA) precoated with mouse monoclonal antibody against Aβ (4G8) or non-immune mouse IgG. We detected bound protein by SELDI time-of-flight mass spectrometry. Calibration was done with synthetic human Aβ1–42 and Aβ1–40.

Immunohistochemistry and staining

Lenses were fixed (0·5% glutaraldehyde 2 h; 4% paraformaldehyde 2 days), embedded in paraffin, and sectioned at 8 μm. We stained the tissue sections with alkaline Congo Red, and examined them with brightfield and cross-polarised light photomicroscopy, or treated them with 90% formic acid, immunostained with monoclonal antibodies against Aβ (4G8 or βA4), and processed them for conventional immunohistochemistry (Vectastain, Vector Laboratories, Burlingame, CA, USA). We did THIOFLAVIN FLUORESCENCE ANALYSIS on 8 μm paraffin-embedded sections stained with 1% thioflavin-S, differentiated in 1% acetic acid, and detected by fluorescence photomicroscopy.

Immunogold electron microscopy

Fixed lenses were cryosectioned and processed for immunogold electron microscopy.[20] We used mouse monoclonal antibodies against Aβ (4G8) or against β-APP (22C11) for immunostaining. Protein aggregates and lens specimens assayed for double anti-Aβ/anti-αB-crystallin immunogold analysis were spotted on carbon-coated hydrophilic grids, incubated with monoclonal antibody 4G8 or non-immune mouse IgG, incubated with rabbit anti-mouse polyclonal antibody (Dako, Carpenteria, CA), and exposed to commercially obtained 15 nm gold-conjugated protein-A (Jan Slot, Utrecht, Netherlands). We fixed grids with 1% glutaraldehyde, quenched them with glycine, incubated them with anti-αB-crystallin polyclonal antibody (J Liang, Brigham and Women's Hospital, Boston, MA, USA) or normal rabbit serum, and exposed the grids to 10 nm gold-conjugated protein-A (Jan Slot). Because of the high concentration of αB-crystallin relative to Aβ in the lens, the anti-αB-crystallin dilution was adjusted to boost visualisation of both proteins. To control for antibody specificity, primary antibodies (monoclonal antibody against Aβ [4G8] and polyclonal antibody against αB-crystallin) were preabsorbed overnight at 4°C with excess antigenic protein—ie, synthetic human Aβ1–40 or recombinant human αB-crystallin, respectively—and briefly centrifuged before use. We negatively stained immunogold electron microscopic specimens with uranyl acetate and examined them on a JEOL 1200EX transmission electron microscope (Jeol USA, Peabody, MA, USA).

ELISA binding assay

We incubated recombinant human αB-crystallin for 1 h at 20°C in 96-well microtitre plates precoated with synthetic human Aβ1–42, synthetic human Aβ1–40, or bovine serum albumin. Bound αB-crystallin was detected by incubation with a rabbit polyclonal antibody then by anti-rabbit horseradish peroxidase conjugate. Bound complex was developed with 3,3′,5,5′-tetramethylbenzidine dihydrochloride.[21] Absorbance (450 nm) was spectrophotometrically assessed (SpectraMax Plus, Molecular Devices, Sunnyvale, CA, USA) and blanked against wells without added αB-crystallin. Datapoints are means (SE) of triplicate measurements.

In-vitro assays

We homogenised intact human lenses in ice-cold, filter-sterilised, analytical-grade HPLC water (Sigma, St Louis, MO, USA) and ultracentrifuged them at 100 000 *g* for 1 h at 4°C. We retained the supernatant as soluble total lens protein. Synthetic human Aβ1–42 was ultrasonically solubilised in HPLC water and centrifuged to remove precipitated material. Incubation mixtures (Aβ1–42, 45 mg/L [10 μmol/L]; total lens protein, 1 g/L) were prepared in sterile chelating resin-treated (Chelex 100, Sigma) phosphate-buffered saline (pH 7·4), plated under sterile conditions in 96-well microtitre plates, sealed, and incubated in the dark for 7 days at 37°C.

Role of the funding source

The sponsors had no role in study design, data collection, data analysis, data interpretation, writing of the report, or in the decision to submit the report for publication.

Results

We first identified and characterised β-APP and Aβ in the adult human lens (figures 1, 2, and 3). We detected full-length β-APP (110 kD and 130 kD) by affinity purification and western blot with monoclonal antibody 6E10, an antibody that detects the Aβ region of β-APP (figure 1). We also detected full-length β-APP in the B3 human lens epithelial cell line and primary human lens epithelial cells by western blot with antibodies against the C-terminal (A8717) and N-terminal (22C11) domains of β-APP (data available from authors). Results of western blot with WO2 (figure 1), a monoclonal antibody against Aβ, showed an

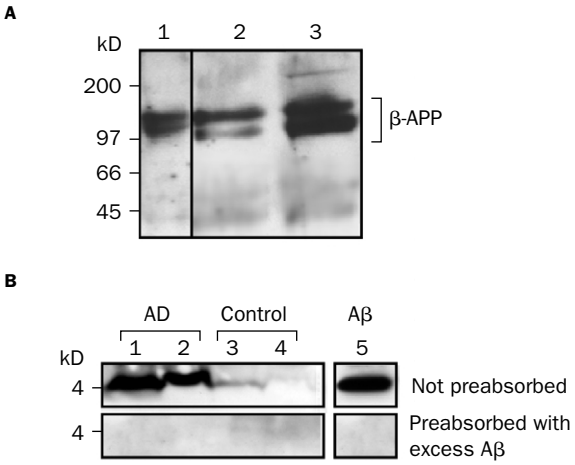

Figure 1: **Western blot analysis of β-APP (A) and Aβ (B) in the human lens and retina**

AD=Alzheimer's disease. (A) Human brain (lane 1), lens (lane 2), and retina (lane 3). β-APP was purified and concentrated by anion exchange chromatography. Antibody used was 6E10. (B) Supernatant (lanes 1 and 3) and urea-resolubilised pellet (lanes 2 and 4) of lens homogenate; synthetic human Aβ1–40 (0·5 ng; lane 5). Antibody used was WO2 (upper) and WO2 preabsorbed with excess synthetic human Aβ1–40 (lower).

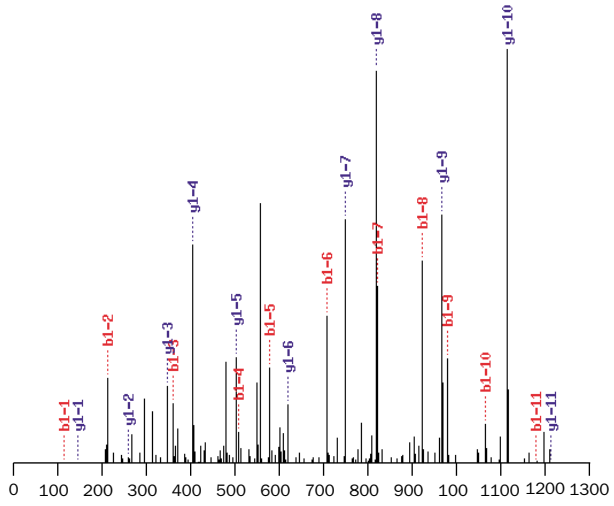

Human Aβ1–42

DAEFRHDSGY EVHHQKLVFF AEDVGSNKGA IIGLMVGGVV IA

Human Aβ1–40

DAEFRHDSGY EVHHQKLVFF AEDVGSNKGA IIGLMVGGVV

Figure 2: **Tryptic digest sequencing/LC-tandem mass spectrometry of the roughly 4 kD band derived from lens homogenate from an adult with Alzheimer's disease**

The identified tryptic peptide corresponds to the Aβ region of β-APP (688–699). A unique 12-residue tryptic peptide derived from the 4 kD band detected by anti-Aβ western blot is highlighted by a black box overlying the human Aβ sequences.

immunoreactive band that migrated at a molecular weight equivalent to apparent monomeric Aβ (about 4 kD). This band was detectable in both the supernatant and urea-resolubilised pellet fractions obtained from human lens protein homogenate derived from patients with and without Alzheimer's disease. We did not detect this approximately 4 kD band when blots were probed with monoclonal antibody WO2 preabsorbed with excess synthetic Aβ (figure 1) or with a polyclonal antibody directed against the C-terminal domain of β-APP (data available from authors). In a small sample of lenses analysed by anti-Aβ western-blot densitometry, a trend towards amplified total monomeric Aβ load was reported in lenses from three individuals with Alzheimer's disease (total monomeric Aβ 3·01, 0·4, 6·17 μg/g protein) relative to lenses from three age-matched controls (0·52, 0·98, 0·53 μg/g protein) when assayed on the same blot.

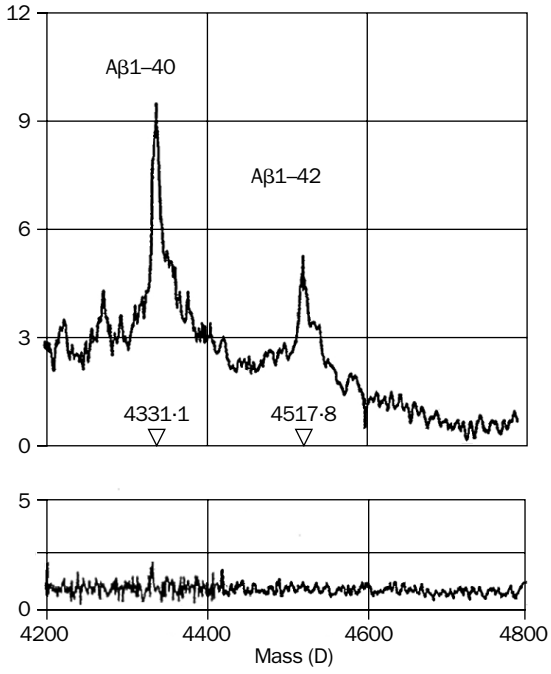

Figure 3: **Anti-Aβ SELDI-mass spectrometry of human lens protein extract**

(Upper) Protein-chip array coated with mouse anti-Aβ 4G8. (Lower) Array precoated with non-immune mouse IgG.

The identity of Aβ in human lens was confirmed by tryptic digestion sequencing with electrospray ionisation LC-tandem mass spectrometry, as shown in figure 2. Analysis of an approximately 4 kD band—excised and sequenced from SDS-PAGE that corresponded to an anti-Aβ western blot of lens extract obtained from an 83-year-old man with severe Alzheimer's disease—yielded a 12-residue tryptic peptide (LVFFAEDVGSNK, molecular weight 1326·49 kD) with two charge states, +2 and +1, that uniquely identified an internal peptide within the Aβ region of β-APP (β-APP688–699). This aminoacid sequence of the identified tryptic peptide is identical in both Aβ1–40 and Aβ1–42. To distinguish these two Aβ isoforms, SELDI mass spectrometry was done on human lens extract from a 56-year-old woman without Alzheimer's disease (figure 3). When the protein-chip array was precoated with the mouse anti-Aβ monoclonal antibody 4G8, we detected two major peaks that corresponded to human Aβ1–40 (observed molecular weight, 4331·1 kD; predicted molecular weight, 4329·9 kD) and Aβ1–42 (observed 4517·8 kD; predicted 4514·1 kD) in a relative mass ratio of about 5/1, respectively. Signals were not seen when array wells were precoated with non-immune mouse IgG or without capture antibody (data available from authors). The detected peaks were identical to those obtained with synthetic human Aβ1–40 and Aβ1–42 and in lens protein extracts spiked with synthetic human Aβ (data available from authors).

Anti-Aβ SELDI mass spectrometry analyses of adult human primary aqueous humour from three people without Alzheimer's disease (79-year-old woman; 74-year-old man; 87-year-old woman) yielded a large peak that corresponded to human Aβ1–40 (mean 29·0 μg/L [SD 12·5]) and a minor peak near the assay detection limit that corresponded to Aβ1–42 (data available from authors). We did not analyse aqueous humour from postmortem specimens due to the susceptibility of this fluid to postmortem changes.

These findings gave us encouragement to do a slit-lamp survey of human lenses obtained from nine people with confirmed Alzheimer's disease neuropathology (five women, four men; mean age 79·1 years [SD 11·0]; mean postmortem interval 15 h [SD 8]) and eight controls (two with frontotemporal dementia; one with progressive supranuclear palsy; one diffuse Lewy body disease with minimum amyloid pathology; three without neurological disease; and one 14-year-old male). Supranuclear cataracts, an uncommon phenotype,[22] were noted in all those with Alzheimer's disease (figure 4), but in none of the controls. These cataracts were typically concentrated in the equatorial region and in some cases extended into deep cortical areas. We noted variation in the extent of opacification, cataract morphology, and comorbid lens pathological findings. We excluded the possibility that the cataracts were artifacts, since we did not see lens swelling, diffuse cloudiness, or other global changes that would indicate organ damage; moreover, postmortem lens changes do not result in focal lens opacification (L T Chylack Jr, unpublished data).

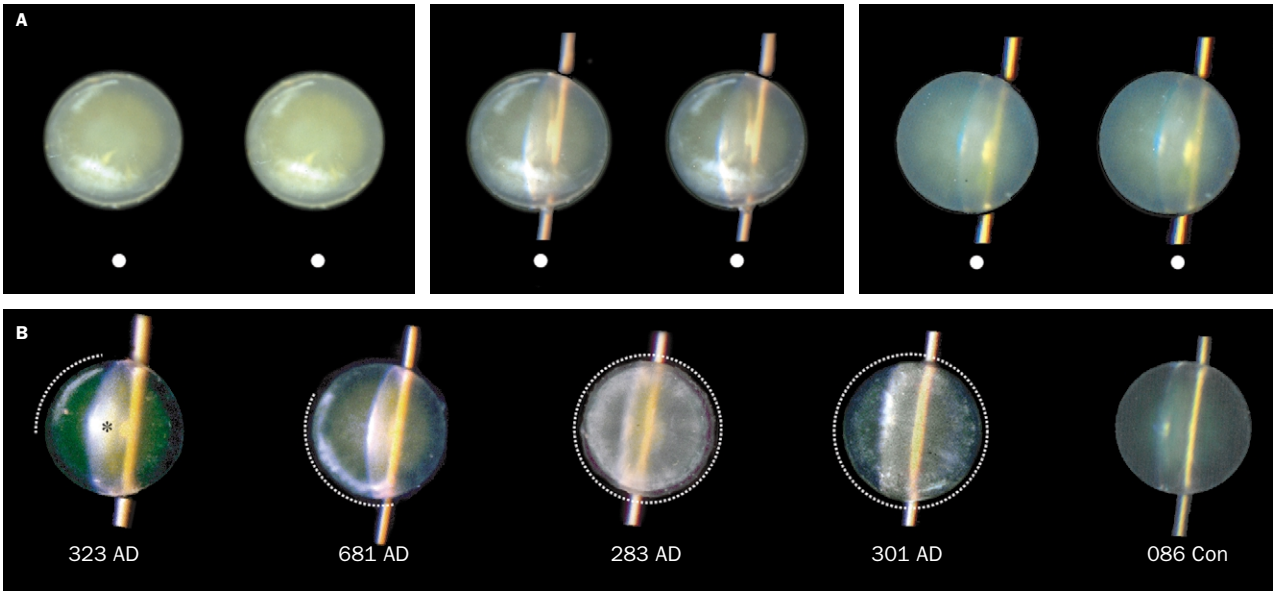

Figure 4: **Slit-lamp survey of lenses from people with Alzheimer's disease and controls**
AD=Alzheimer's disease. Con=control. (A) Stereoscopic photomicrographs of one lens from an 80-year-old woman with severe Alzheimer's disease without (left) and with (middle) slit-lamp illumination. Visual convergence of white dots indicates stereoscopy. Supranuclear cataracts are present in the superior and inferior left-hand quadrants. Control lens from an 80-year-old woman without Alzheimer's disease (right) without supranuclear cataracts. (B) Dashed arc or circle indicates extent of supranuclear cataract. In lens 323 (79-year-old woman), asterisk represents nuclear cataract. Lens 086 (from a 63-year-old woman with frontotemporal dementia and Parkinson's disease) shows no evidence of supranuclear or cortical cataracts. Lens 681 from a 68-year-old woman; lens 283 from an 82-year-old woman; and lens 301 from a 72-year-old woman.

We did histological analysis of lenses obtained from age-matched individuals with (n=4) and without (n=4) Alzheimer's disease (figure 5). Lenses from people with the disorder showed Aβ-immunostaining in the supranuclear and cortical lens subregions. Congo Red staining revealed dichroism and red-green birefringence when viewed under strong cross-polarised light, tinctorial properties that are pathognomonic of amyloid. This birefringent staining was seen in the same regions that showed Aβ immunostaining. We also noted artifactual Congo Red staining of collagen in the lens capsule that did not show anti-Aβ immunostaining. Intense thioflavin-S fluorescence was also seen in the same supranuclear and deep cortical lens regions in which we detected Aβ-immunoreactivity and birefringent Congo Red staining (data available from authors). Assessment of elderly control lens showed faint Aβ immunoreactivity in the supranuclear and deep cortical lens regions. The superficial cortical regions in control lens showed congophilia with minimum birefringence. In the specimens from people with Alzheimer's disease, lens regions showing strong Aβ-immunoreactivity and Congo Red staining accorded with the same supranuclear and deep cortical areas in which cataracts were identified by slit-lamp examination (figure 5, G).

Analysis of Alzheimer's disease lens specimens (n=4) by anti-Aβ immunogold electron microscopy (figure 5) showed abundant clusters of electron-dense Aβ-immunoreactive material that localised exclusively to the lens fibre-cell cytoplasm. Aβ immunoreactivity was not seen in classic amyloid fibrils, extracellular regions, membrane-

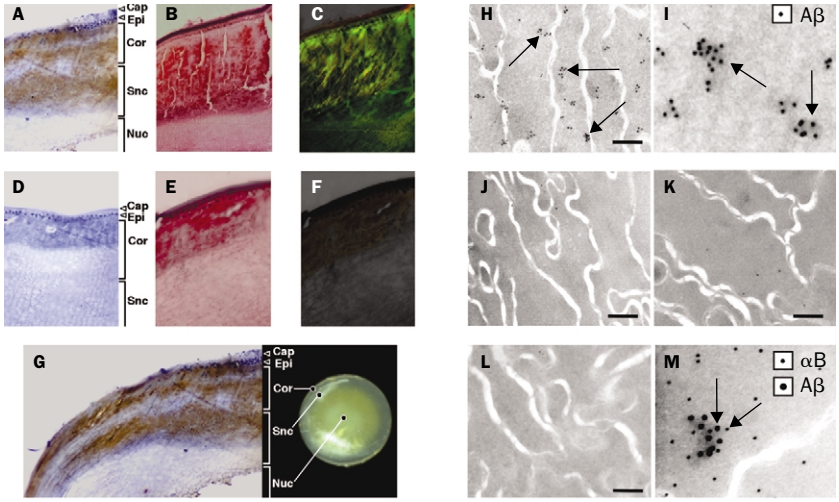

Figure 5: **Histological analysis (A–G) and ultrastructural characterisation (H–M) of lenses from people with Alzheimer's disease and controls**
(A) Anti-Aβ immunostaining of lens from an 80-year-old woman with Alzheimer's disease. (B) Congo Red staining and (C) red-green birefringence in same lens. (D) Faint anti-Aβ immunostaining in control lens from an 80-year-old woman without Alzheimer's disease. (E) Congo Red staining and (F) faint birefringence in same control lens. (G) Correlation of histological localisation of Aβ and cataract pathology in Alzheimer's disease lens. (H) Anti-Aβ immunogold electron photomicrograph of deep cortical region of lens from an 82-year-old woman with Alzheimer's disease. (H) Black arrows show anti-Aβ-immunoreactive clusters present exclusively within the lens fibre-cell cytoplasm. Scale bar=200 nm. (I) Higher magnification of same lens section showing the enhanced electron-density of the cytosolic Aβ-immunoreactive aggregates (black arrows). (J) Anti-Aβ immunogold electron photomicrograph of deep cortical region of control lens from a 76-year-old woman without Alzheimer's disease. Scale bar=200 nm. (K, L) Absence of immunostaining in the lens specimen from the individual in H and I probed with anti-Aβ 4G8 preabsorbed with excess synthetic human Aβ (K) or anti-β-APP 22C11 (L). Scale bars=200 nm. (M) Alzheimer's disease lens showing double immunogold staining for Aβ and αB-crystallin within one electron-dense cytosolic aggregate. Larger (15 nm) and smaller (10 nm) gold particles detect Aβ and αB-crystallin immunoreactivity, respectively. Cap=capsule; epi=epithelium; cor=cortex; snc=supranucleaus; nuc=nucleus.

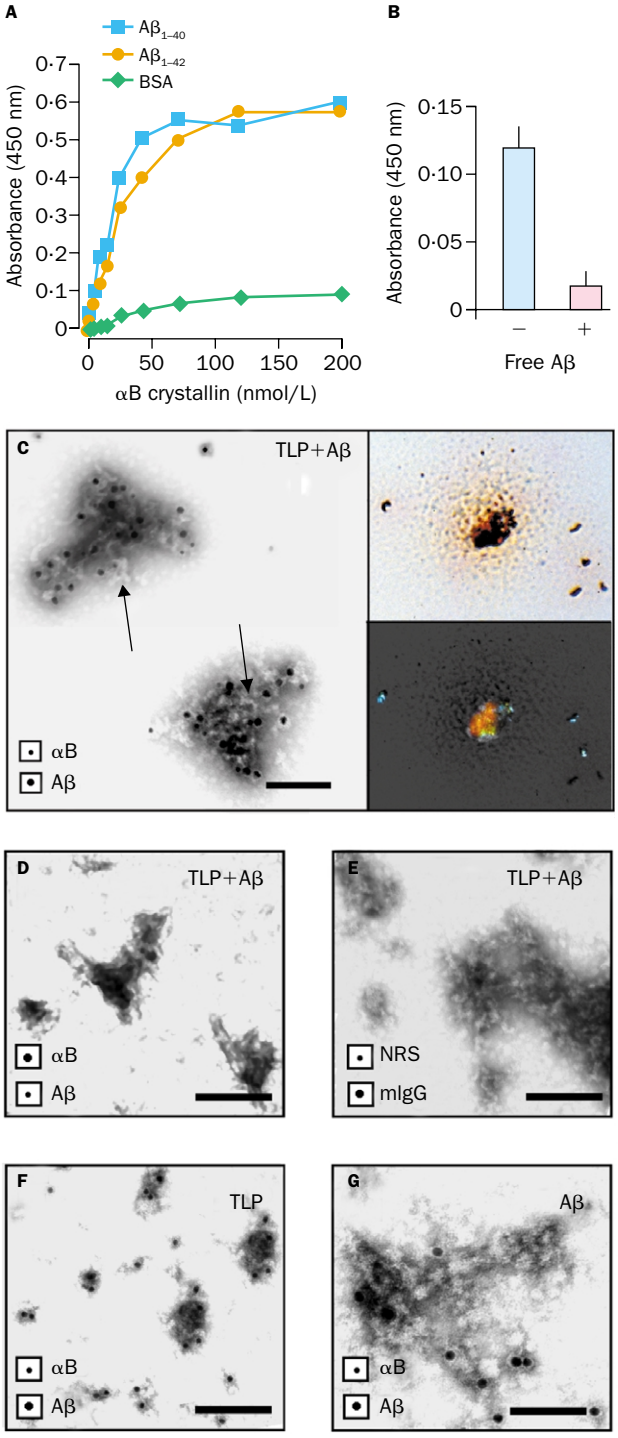

Figure 6: **Aβ and human lens protein interactions**
(A) Binding of recombinant human αB-crystallin to immobilised synthetic human Aβ1–42, synthetic human Aβ1–40, or bovine serum albumin (BSA). (B) Binding competition by addition of excess free Aβ. Bars are mean. Error bars are SE. (C) Human total lens protein (TLP) coincubated with synthetic human Aβ1–42 for 7 days and analysed by anti-Aβ/anti-αB-crystallin double immunogold electron microscopy. Black arrows indicate protofibrils. (C, inset) Precipitated aggregates stained with Congo Red and viewed by brightfield (C, upper) or cross-polarised light (C, lower) showing red-green birefringence. (D) TLP coincubated with synthetic human Aβ1–42 and analysed by anti-Aβ/anti-αB-crystallin double immunogold electron microscopy with primary antibodies preabsorbed with excess Aβ1–40 and αB-crystallin. (E) TLP coincubated as in D and assayed with non-immune mouse IgG (mIgG) and rabbit serum (NRS). (F) TLP incubated without Aβ and assayed as in C. (G) Synthetic human Aβ1–42 incubated without TLP and assayed as in C. Boxes in the figures show gold particle size (to scale). Scale bars=100 nm.

associated material, or in the lens epithelium. Age-related sclerosis prevented investigation of the lens nucleus. Minimum Aβ immunoreactivity was detected in human lens fibre cells from elderly controls. Aβ immunoreactivity was not seen in a control lens from a healthy 14-year-old male or in the B3 human lens epithelial cell line (data available from authors). Preabsorption of the antibody with excess synthetic human Aβ (figure 5) or exclusion of the primary anti-Aβ antibody (data available from authors) abolished immunostaining in lens sections from people with Alzheimer's disease. Sections probed with monoclonal antibody 22C11 directed at the N-terminal ectodomain of β-APP (figure 5), non-immune antibody, or secondary antibody alone (data available from authors) similarly did not show fibre cell anti-Aβ immunoreactivity.

We reasoned that some of the Aβ-immunoreactive deposits we detected might coaggregate with other cytosolic lens proteins such as αB-crystallin. In support of this hypothesis, electron-dense cytosolic aggregates were detected that showed immunoreactivity to both Aβ and αB-crystallin (figure 5). This finding prompted us to investigate the interaction of Aβ with αB-crystallin in vitro. Saturable high-affinity binding was recorded (Kapp about 20 nmol/L) that was competitively inhibited by addition of excess soluble Aβ (figure 6). We reasoned that this binding and the potent pro-oxidant properties of Aβ could, over time, promote lens-protein aggregation within the fibre-cell cytosol. We investigated this possibility by incubation of human total lens protein extract with synthetic human Aβ1–42 for 7 days and analysis of the resulting mixtures by anti-Aβ/anti-αB-crystallin double immunogold electron microscopy. Formation of electron-dense aggregates was noted (figure 6) that were similar to those detected in the ex-vivo lens specimens from people with Alzheimer's disease. Single aggregates showed both Aβ and αB-crystallin immunoreactivity, birefringent Congo Red staining (figure 6), and amplified thioflavin-S fluorescence (data available from authors) indicative of amyloid. These aggregates also showed curvilinear protofibrillar structures[23] but not classic Aβ fibrils. Double immunogold electron microscopic analysis with primary monoclonal antibodies preabsorbed with excess Aβ and αB-crystallin, or non-immune mouse IgG and normal rabbit serum did not result in immunogold staining (figure 6). These data suggest our results were not attributable to non-specific staining artifact. Total lens protein or Aβ incubated alone showed only single-label immunostaining for αB-crystallin or Aβ, respectively.

Discussion

We have identified Aβ1–42 and Aβ1–40 in the human lens and Aβ1–40 in human primary aqueous humour. Our findings show that concentrations of Aβ1–42 and Aβ1–40 in the human lens, and Aβ1–40 in primary human aqueous humour, are comparable with those in aged human cerebral cortex and cerebrospinal fluid, respectively.[24] We also noted increased deposition of electron-dense Aβ-immunoreactive aggregates within lens fibre-cell cytoplasm in the supranuclear subregion of lenses from people with Alzheimer's disease.

The cytosolic localisation of lenticular Aβ is important, since this peptide localises to the same cellular compartment as the highly concentrated crystallins within the lens fibre cell. These cells have limited ability to turn over protein as the lens ages. Thus, lens Aβ is in a position to foster cytosolic lens protein aggregation. This hypothesis is lent support by our evidence from double immunogold electron microscopic examination of lenses from people with Alzheimer's disease showing Aβ and αB-crystallin

immunoreactivity within single cytosolic aggregates and by results presented in this study showing high-affinity binding and coaggregation of Aβ and αB-crystallin.

Although other investigators have noted Aβ within other intracellular compartments,[25,26] the finding of this peptide in the cytoplasm proper was unexpected. The mechanism by which Aβ accumulates in this compartment is unclear. The cytosolic localisation of Aβ in the lens could result from release of this peptide from other intracellular compartments during terminal differentiation of lens epithelial-cell as they mature into long-lived, post-mitotic lens fibre cells. During this process, epithelial cells on the anterior surface of the lens migrate to the equatorial germinative zone and there undergo elongation, nuclear and organellar disintegration, and cessation of protein synthesis. β-APP and its metabolic products, including Aβ, might be initially contained within organelles implicated in β-APP processing—ie, endoplasmic reticulum, Golgi apparatus, and trans-Golgi network. Because these organelles disintegrate during terminal differentiation, Aβ might be released into the cytosol. An alternative explanation invokes endocytic Aβ reinternalisation, a clearance pathway that has been proposed as a possible initiation site for accumulation of Aβ in the brain.[27] This latter mechanism accords with the presence of Aβ in primary aqueous humour. The origin and fate of Aβ in the supranuclear lens fibre cells and in the anterior chamber remain to be established.

Because of the anatomically circumscribed accumulation of Aβ within the lens, our quantitative analysis might have underestimated local Aβ tissue concentration in the supranuclear lens subregion. A more extensive quantitative Aβ analysis done on microdissected lens specimens is underway.

A limitation of this study is the small sample sizes. Nevertheless, our findings do provide evidence for extracerebral Alzheimer's disease-associated amyloid pathology.[28] In particular, we have seen apparent Aβ-related amyloid pathological findings in the equatorial supranuclear and deep cortical subregions of lenses from people with Alzheimer's disease. It is noteworthy that equatorial supranuclear cataracts in this peripheral lens subregion are rare[22] compared with common age-related cataracts. By contrast with age-related cataracts, equatorial supranuclear cataracts are anatomically obscured from inspection by the iris, and are thus neither apparent on routine medical examination nor associated with visual impairment.

We postulate that a relation exists between our finding of Aβ-immunoreactive cytosolic microaggregates in the cytoplasm of supranuclear lens fibre cells and cataract formation in the same lens subregion. Within the lens fibre-cell cytoplasm, electron-dense aggregates—such as those we saw in the lenses from people with Alzheimer's disease—represent sharp discontinuities in the local refractive index. Since small refractive index fluctuations result in very large increases in local light scattering,[29,30] we postulate that Aβ-mediated lens protein aggregation might contribute to the increased light scattering we detected as supranuclear cataracts in lens specimens from people with Alzheimer's disease. This hypothesis is lent support by results of other studies that show protein-protein interactions between Aβ and αB-crystallin.[11–13]

Longevity of expressed protein in the lens fibre cells, the inefficient protein turnover capacity of mature lens fibre cells, and optical accessibility of the lens from the periphery suggest that Aβ deposition in the lens might promote regionally-specific lens protein aggregation that could be detectable throughout the course of Alzheimer's disease. Further exploration of this hypothesis and assessment of the putative association between Alzheimer's disease and supranuclear cataracts awaits controlled ophthalmological studies in people at progressive stages in the Alzheimer's disease process.

Contributors

L E Goldstein, L T Chylack Jr, and A I Bush designed and coordinated the study. L E Goldstein obtained the clinical specimens. L T Chylack Jr classified the lens images. Experimental analyses were done by L E Goldstein, J A Muffat, R A Cherny, R D Moir, M H Ericsson, K A Fitch, X Huang, C Mavros, J A Coccia, and K Y Faget. Data were analysed and interpreted by L E Goldstein, J A Muffat, R A Cherny, R D Moir, X Huang, C L Masters, R E Tanzi, L T Chylack Jr, and A I Bush. The report was written by L E Goldstein, L T Chylack Jr, and A I Bush. L T Chylack Jr and A I Bush contributed equally.

Conflict of interest statement

L E Goldstein and L T Chylack Jr are board members, consultants to, and shareholders in Neuroptix Corporation. A I Bush is a consultant to and shareholder in Prana Biotechnology. C L Masters is a board member, consultant to, and shareholder in Prana Biotechnology.

Acknowledgments

We thank K Obrock and J Growdon (Neurology), T Hedley-Whyte, I Delalle, K Newell, and R Pfannl (Neuropathology), J Tarelli, S Conley, and M Forrestal (Pathology), M Albert (Psychiatry), and the Massachusetts Alzheimer's Disease Research Center (National Institute on Aging grant AG005134-19), at the Massachusetts General Hospital; J Liang and D Hartley (Brigham and Women's Hospital); R Pineda (Massachusetts Eye and Ear Infirmary); J Horwitz (UCLA School of Medicine); I Volitakis (University of Melbourne); B Alpert (Micro Video Instruments, Avon, MA, USA); New England Eye and Tissue Bank (Boston); National Disease Registry Interchange (Philadelphia); and the families who donated tissues to make this research possible. This work is supported by grants from the Rappaport Foundation to LEG; National Institute on Aging (AG12686), Alzheimer's Association, and NHMRC (Australia) to AIB; and Massachusetts Lions Eye Research Foundation to LTC.

References

1 Kang J, Lemaire HG, Unterbeck A, et al. The precursor of Alzheimer's disease amyloid A4 protein resembles a cell-surface receptor. *Nature* 1987; **325:** 733–36.
2 Tanzi RE, Bertram L. New frontiers in Alzheimer's disease genetics. *Neuron* 2001; **32:** 181–84.
3 Butterfield DA, Lauderback CM. Lipid peroxidation and protein oxidation in Alzheimer's disease brain: potential causes and consequences involving amyloid beta-peptide-associated free radical oxidative stress. *Free Radic Biol Med* 2002; **32:** 1050–60.
4 Hanson SR, Hasan A, Smith DL, Smith JB. The major in vivo modifications of the human water-insoluble lens crystallins are disulfide bonds, deamidation, methionine oxidation and backbone cleavage. *Exp Eye Res* 2000; **71:** 195–207.
5 Spector A. Oxidation and cataract. *Ciba Found Symp* 1984; **106:** 48–64.
6 Lowe RF. The eyes in mongolism. *Br J Ophthalmol* 1949; **33:** 131–74.
7 Holton JL, Lashley T, Ghiso J, et al. Familial Danish dementia: a novel form of cerebral amyloidosis associated with deposition of both amyloid-Dan and amyloid-beta. *J Neuropathol Exp Neurol* 2002; **61:** 254–67.
8 Frederikse PH, Garland D, Zigler JSJ, Piatigorsky J. Oxidative stress increases production of beta-amyloid precursor protein and beta-amyloid (Aβ) in mammalian lenses, and Aβ has toxic effects on lens epithelial cells. *J Biol Chem* 1996; **271:** 10169–74.
9 Horwitz J. The function of alpha-crystallin in vision. *Semin Cell Dev Biol* 2000; **11:** 53–60.
10 Lowe J, Errington DR, Lennox G, et al. Ballooned neurons in several neurodegenerative diseases and stroke contain αB crystallin. *Neuropathol Appl Neurobiol* 1992; **18:** 341–50.
11 Stege GJ, Renkawek K, Overkamp PS, et al. The molecular chaperone alphaB-crystallin enhances amyloid beta neurotoxicity. *Biochem Biophys Res Commun* 1999; **262:** 152–56.
12 Liang JJ. Interaction between beta-amyloid and lens alphaB-crystallin. *FEBS Lett* 2000; **484:** 98–101.
13 Fonte V, Kapulkin V, Taft A, Fluet A, Friedman D, Link CD. Interaction of intracellular beta amyloid peptide with chaperone proteins. *Proc Natl Acad Sci U S A* 2002; **99:** 9439–44.
14 Harding JJ. Alzheimer disease and cataract: common threads. *Alz Dis Assoc Dis* 1997; **11:** 123.

15 Bush AI, Goldstein LE. Specific metal-catalysed protein oxidation reactions in chronic degenerative disorders of ageing: focus on Alzheimer's disease and age-related cataracts. *Novartis Found Symp* 2001; **235:** 26–38.
16 Mirra SS, Heyman A, McKeel D, et al. The Consortium to Establish a Registry for Alzheimer's Disease (CERAD), part II: standardization of the neuropathologic assessment of Alzheimer's disease. *Neurology* 1991; **41:** 479–86.
17 Chylack LT Jr. Classification of human cataractous change by the American Cooperative Cataract Research Group method. *Ciba Found Symp* 1984; **106:** 3–24.
18 Moir RD, Lynch T, Bush AI, et al. Relative increase in Alzheimer's disease of soluble forms of cerebral Abeta amyloid protein precursor containing the Kunitz protease inhibitory domain. *J Biol Chem* 1998; **273:** 5013–19.
19 Cherny RA, Legg JT, McLean CA, et al. Aqueous dissolution of Alzheimer's disease Abeta amyloid deposits by biometal depletion. *J Biol Chem* 1999; **274:** 23223–28.
20 Griffiths G. Fine structure immunocytochemistry. Heidelberg: Springer Verlag, 1993.
21 Moir RD, Atwood CS, Romano DM, et al. Differential effects of apolipoprotein E isoforms on metal-induced aggregation of Aβ using physiological concentrations. *Biochem* 1999; **38:** 4595–603.
22 Chylack LT Jr, White O, Tung WH. Classification of human senile cataractous change by the American Cooperative Cataract Research Group (CCRG) method: II, staged simplification of cataract classification. *Invest Ophthalmol Vis Sci* 1984; **25:** 166–73.
23 Hartley DM, Walsh DM, Ye CP, et al. Protofibrillar intermediates of amyloid beta-protein induce acute electrophysiological changes and progressive neurotoxicity in cortical neurons. *J Neurosci* 1999; **19:** 8876–84.
24 McLean CA, Cherny RA, Fraser FW, et al. Soluble pool of Aβ amyloid as a determinant of severity of neurodegeneration in Alzheimer's disease. *Ann Neurol* 1999; **46:** 860–66.
25 Skovronsky DM, Doms RW, Lee VM. Detection of a novel intraneuronal pool of insoluble amyloid beta protein that accumulates with time in culture. *J Cell Biol* 1998; **141:** 1031–39.
26 Gouras GK, Tsai J, Naslund J, et al. Intraneuronal Aβ42 accumulation in human brain. *Am J Pathol* 2000; **156:** 15–20.
27 Glabe C. Intracellular mechanisms of amyloid accumulation and pathogenesis in Alzheimer's disease. *J Mol Neurosci* 2001; **17:** 137–45.
28 Joachim CL, Mori H, Selkoe DJ. Amyloid beta-protein deposition in tissues other than brain. *Nature* 1989; **341:** 226–30.
29 Benedek GB. Theory of transparency of the eye. *Applied Optics* 1971; **10:** 459–73.
30 Vaezy S, Clark JI. A quantitative analysis of transparency in the human sclera and cornea using Fourier methods. *J Microsc* 1991; **163:** 85–94.

10 most wanted

Introducing the most wanted *Lancet* articles

January, 2003

1 Bone-marrow transplantation for the heart—myocardial regeneration (Jan 4, 2003)
Stamm C, Westphal B, Kleine H-D, et al. Autologous bone-marrow stem-cell transplantation for myocardial regeneration. DOI:10.1016/S0140-6736(03)12110-1. *Lancet* 2003; **361:** 45–46.

2 COOPERATion (Jan 11, 2003)
Nakao N, Yoshimura A, Morita H, Takada M, Kayano T, Ideura T. Combination treatment of angiotensin-II receptor blocker and angiotensin-converting-enzyme inhibitor in non-diabetic renal disease (COOPERATE): a randomised controlled trial. DOI:10.1016/S0140-6736(03)12229-5. *Lancet* 2003; **361:** 117–24.

3 PTCA wins over thrombolytic therapy in AMI (Jan 4, 2003)
Keeley EC, Boura JA, Grines CL. Primary angioplasty versus intravenous thrombolytic therapy for acute myocardial infarction: a quantitative review of 23 randomised trials. DOI:10.1016/S0140-6736(03)12113-7. *Lancet* 2003; **361:** 13–20.

4 Common cold (Jan 4, 2003)
Heikkinen T, Järvinen A. The common cold. DOI:10.1016/S0140-6736(03)12162-9. *Lancet* 2003; **361:** 51–59.

5 Dementia explained (Nov 30, 2002)
The dementias. Ritchie K, Lovestone S. DOI:10.1016/S0140-6736(02)11667-9. *Lancet* 2002; **360:** 1759–66.

6 Myocardial regeneration in context (Jan 4, 2003)
Bone-marrow transplantation for the heart: fact or fiction?. Laham RJ, Oettgen P. DOI:10.1016/S0140-6736(03)12186-1. *Lancet* 2003; **361:** 11–12.

7 Bone-marrow transplantation for the heart—angiogenesis (Jan 4, 2003)
Tse H-F, Kwong Y-L, Chan JKF, Lo G, Ho C-L, Lau C-P. Angiogenesis in ischaemic myocardium by intramyocardial autologous bone marrow mononuclear cell implantation. DOI:10.1016/S0140-6736(03)12111-3. *Lancet* 2003; **361:** 47–49.

8 Protecting the heart (July 6, 2002)
Heart Protection Study Collaborative Group. MRC/BHF Heart Protection Study of cholesterol lowering with simvastatin in 20 536 high-risk individuals: a randomised placebo-controlled trial. doi:10.1016/S0140-6736(02)09327-3. *Lancet* 2002; **360:** 7–22.

9 Concern over dietary supplements (Jan 11, 2003)
Palmer ME, Haller C, McKinney PE, et al. Adverse events associated with dietary supplements: an observational study. DOI:10.1016/S0140-6736(03)12227-1. *Lancet* 2003; **361:** 101–06.

10 Time to PROSPER (Nov 23, 2002)
Shepherd J, Blauw GJ, Murphy MB, et al, on behalf of the PROSPER study group. Pravastatin in elderly individuals at risk of vascular disease (PROSPER): a randomised controlled trial. DOI:10.1016/S0140-6736(02)11600-X. *Lancet* 2002; **360:** 1759–66.

The Science Citation Index (SCI), calculated on the basis of citations that a paper receives after publication, is one measure (albeit a controversial one) of the value of that paper. SCI data, which are used to create *Science Watch*'s infamous Hot Papers, are avidly digested by scientists (and the journals in which they publish), so the SCI is also a proxy for usage. The web has transformed access to information; instant retrieval with a few clicks of a mouse means that it is increasingly the preferred source of scientific information. The web, therefore, provides another measure of usage. This week, *The Lancet* starts its own score-keeping of downloaded articles as requested by users of ScienceDirect (http://www.sciencedirect.com), Elsevier's web database of more than 1700 science, medical, and technical peer-reviewed journals, of which *The Lancet* is one. We start this monthly column with the 10 most wanted *Lancet* articles downloaded during the month of January, 2003.

Pia Pini
***The Lancet*, London, UK**